Direct-Drive Inertial Confinement Fusion Research at the Laboratory for Laser Energetics: Charting the Path to Thermonuclear Ignition

R.L. McCrory 1), S.P. Regan 1), S.J. Loucks 1), D.D. Meyerhofer 1), S. Skupsky 1), R. Betti 1), T.R. Boehly 1), R.S. Craxton 1), T.J.B. Collins 1), J.A. Delettrez 1), D. Edgell 1), R. Epstein 1), K.A. Fletcher 3), C. Freeman 3), J.A. Frenje 2), V.YU. Glebov 1), V.N. Goncharov 1), D.R. Harding 1), R.L. Keck 1), J.P. Knauer 1), C.K. Li 2), J. Marciante 1), J.A. Marozas 1), F.J. Marshall 1), A.V. Maximov 1), P.W. McKenty 1), J. Myatt 1), S. Padalino 3), R.D. Petrasso 2), P.B. Radha 1), T.C. Sangster 1), F. H. Séguin 2), W. Seka 1),V.A. Smalyuk 1), J.M. Soures 1), C. Stoeckl 1), B. Yaakobi 1), and J.D. Zuegel 1)

1) Laboratory for Laser Energetics, University of Rochester, Rochester, NY, USA
2) Plasma Science and Fusion Center, MIT, Cambridge, MA, USA
3) SUNY Geneseo, Geneseo, NY, USA

E-mail address of main author: rmcc@lle.rochester.edu

Abstract: Significant theoretical and experimental progress continues to be made at the University of Rochester's Laboratory for Laser Energetics (LLE), charting the path to direct-drive ignition. Direct-drive inertial confinement fusion (ICF) offers the potential for higher-gain implosions than x-ray drive and is a leading candidate for an inertial fusion energy power plant. LLE's direct-drive ICF ignition target designs for the National Ignition Facility (NIF) are based on hot-spot ignition. A cryogenic target with a spherical DT-ice layer, within or without a foam matrix, enclosed by a thin plastic shell, is directly irradiated with ~1.5 MJ of laser energy. Cryogenic and plastic/foam (surrogate-cryogenic) targets that are hydrodynamically scaled from ignition target designs are imploded on the OMEGA 60-beam, 30-kJ, UV laser system to investigate the key target physics issues of energy coupling, hydrodynamic instabilities, and implosion symmetry. Cryogenic D_2-ice-layer finishes approaching the 1-μm NIF requirement have been produced. Prospects for direct-drive ignition on the NIF are extremely favorable, even while it is configured in its x-ray-drive irradiation configuration with polar direct-drive (PDD). A high-energy petawatt capability is being constructed at LLE next to the existing 60-beam OMEGA compression facility. The OMEGA EP (extended performance) laser will add two short-pulse, 2- to 3-PW, 2.6-kJ beams to the OMEGA laser system to study fast-ignition physics with focused intensities up to 6×10^{20} W/cm^2.

1. Introduction

The goal of thermonuclear ignition and high gain in the laboratory with direct-drive inertial confinement fusion (ICF) requires a physical understanding of the entire implosion process. Significant theoretical and experimental progress charting this path to ignition continues to be made at the University of Rochester's Laboratory for Laser Energetics (LLE). Direct-drive ICF offers the potential for higher-gain implosions than x-ray drive and is a leading candidate for an inertial fusion energy power plant [1].

LLE's direct-drive ICF ignition target designs for the National Ignition Facility (NIF) rely on hot-spot ignition [2], where a cryogenic target with a spherical DT-ice layer, within or without a foam matrix, enclosed by a thin plastic shell will be directly irradiated with ~1.5 MJ of laser energy [3]. The NIF, currently under construction at the Lawrence Livermore National Laboratory, is a 1.8-MJ, 351-nm, 192-beam laser system [4]. During the implosion the main fuel layer will compress the DT gas, forming a central hot spot. A thermonuclear burn wave is predicted to propagate through the main fuel layer when the fuel areal density of the hot spot reaches ~0.3 g/cm^2 with a temperature of ~10 keV [2,5]. Our research shows that high-gain (~35) ignition with the baseline direct-drive target design on the NIF is likely [6].

The path to ignition is being explored with (hydrodynamically) scaled direct-drive-implosion experiments on the 60-beam, 30-kJ OMEGA laser system [7]. These experiments are validating the hydrodynamics codes used to design the NIF high-gain, cryogenic DT targets. The targets are imploded on OMEGA to investigate the key target physics issues of energy coupling, hydrodynamic instabilities, and implosion symmetry. The performance of imploding cryogenic D_2 capsules on OMEGA is close to the predictions of the 2-D hydrodynamics code *DRACO* [5]. This research gives high confidence that direct-drive implosions will ignite on the NIF with symmetric illumination.

NIF will be initially configured for x-ray drive, which has no equatorial beams to symmetrically irradiate a direct-drive target. Although the implementation of the direct-drive beam configuration is not scheduled until 2014, prospects for direct-drive ignition on the NIF while it is in its x-ray-drive irradiation configuration are favorable with polar direct-drive (PDD) [8]. The PDD target design currently has a 2-D predicted gain of ~10. PDD simulations are being validated by experiments on OMEGA.

A complementary approach to hot-spot ignition, namely fast ignition (FI) [9] is also an active area of research at LLE. A high-energy petawatt capability is being constructed at LLE next to the existing OMEGA compression facility. The OMEGA EP (extended performance) laser will add two short-pulse, 2- to 3-PW, 2.6-kJ beams to the OMEGA laser system to study FI physics with focused intensities up to 6×10^{20} W/cm^2 for experiments beginning in 2008. Direct-drive fuel assembly experiments with FI cone targets have begun on OMEGA, and a substantial fraction of the predicted core areal density has been measured.

This paper provides an overview of the direct-drive target physics program at LLE. A general description of direct-drive ICF and the techniques used to mitigate the effects of hydrodynamic instabilities is given in Sec. 2. Symmetric direct-drive implosions of high-performance scaled cryogenic targets on OMEGA and the predicted performance of LLE's baseline direct-drive target design for the NIF are presented in Sec. 3. PDD for the NIF and PDD experiments on OMEGA are discussed in Sec. 4. A brief description of the OMEGA EP is given in Sec. 5, along with the results from FI fuel assembly experiments.

2. Direct-Drive Inertial Confinement Fusion

A direct-drive implosion is initiated by the ablation of material from the outer surface of a spherical shell containing thermonuclear fuel with intense laser beams [6]. The ablated shell mass forms a coronal plasma that surrounds the target and accelerates the shell inward via the rocket effect [2]. Since ICF target acceleration and subsequent deceleration are realized when hot, low-density plasma pushes against cold, high-density plasma, the target implosion is unstable to the Rayleigh–Taylor instability (RTI) [2,6,10]. The implosion can be divided into four stages: early time, acceleration phase, deceleration phase, and peak compression. Perturbation seeds early in the implosion from laser imprint, laser drive asymmetry, and the outer/inner shell surface roughness determine the final capsule performance. The unstable RTI growth is controlled by reducing the seeds (e.g., laser imprint and target surface roughness) and the growth rates of the dominant modes. These perturbations feed through the shell during the acceleration phase and seed the RTI of the deceleration phase at the inner shell surface [11]. When the higher-density shell converges toward the target center and is decelerated by the lower-density hot-spot plasma, the RTI causes mixing of the shell material with the hot spot (i.e., shell mix) [12]. Modulations also grow due to Bell–Plesset convergent effects throughout the implosion [13,14]. The thermonuclear fusion rate increases as the compression heats the hot spot and increases its fuel areal density. Predictions show that alpha-particle heating causes a thermonuclear burn wave to propagate through the main fuel layer when the fuel areal density of the central hot spot reaches ~0.3 g/cm^2 with a temperature of ~10 keV [2,5]. Ultimately, the RTI can disrupt the central hot spot formation and prevent it from igniting. An understanding of the RTI-induced mix and developing ways to control it are of great importance for the goal of achieving thermonuclear ignition in the laboratory.

The target physics research program at LLE combines all aspects of direct-drive ICF including early-time phenomena such as plasma formation and laser-beam imprinting, RTI growth during the acceleration and deceleration phases, shell mix at peak burn, and shock timing and coalescence. High-performance cryogenic and mass equivalent gas-filled plastic shell (i.e., warm surrogate) implosions are studied. Surrogate targets are used to develop an understanding of the physics of capsule implosions without being encumbered by the technological complications associated with cryogenic targets. Target performance is diagnosed with neutronics [15], charged-particle spectroscopy [16,17], x-ray spectroscopy [18], and x-ray imaging [19]. OMEGA creates extreme states of matter with high reproducibility. An example of such performance is shown in Fig. 1, which presents the measured primary neutron yield over the last four years on OMEGA of a benchmark implosion of a 15-atm, deuterium-filled, 20-μm-thick plastic-shell target irradiated with a 23-kJ, 1-ns-square laser pulse.

Laser imprint levels are reduced by creating a uniform laser irradiation of the target. High-compression direct-drive experiments require a 1% rms level of on-target laser irradiation nonuniformity averaged over a few hundred picoseconds [20]. This is accomplished on the OMEGA laser system using two-dimensional smoothing by spectral dispersion (2-D SSD) [21–23], distributed phase plates (DPP's) [24,25], polarization smoothing (PS) utilizing birefringent wedges [26–28], and multiple-beam overlap [29]. These techniques have been demonstrated on OMEGA [30] and are directly applicable to direct-drive ignition target designs planned for the NIF [5].

The low ℓ-mode laser irradiation uniformity was recently improved on OMEGA with a new phase-plate design along with improvements in beam pointing, beam balance, and target-positioning accuracy [29]. The envelope of the single beam far field intensity has a super-Gaussian shape, $I(r) \propto \exp\left[-(r/\delta)^n\right]$, where r is the radius of the beam, δ is the 1/e-half-width, and n is the super-Gaussian order. The new SG4 phase-plate design with $n = 4.1$ replaced the SG3 design with $n = 2.2$, resulting in a reduction in the on-target laser-irradiation nonuniformities for $\ell \leq 10$ by almost a factor of two. The effects of the low-ℓ-mode nonuniformities on the target performance of high-adiabat, deuterium-filled-plastic-shell implosions were investigated. Implosions are categorized by the adiabat α or isentrope parameter of the shell, which is defined as the ratio of the shell pressure to the Fermi-degenerate pressure. Target performance is quantified by the ratio of measured primary neutron yield to 1-D predicted yield, which is defined as the yield

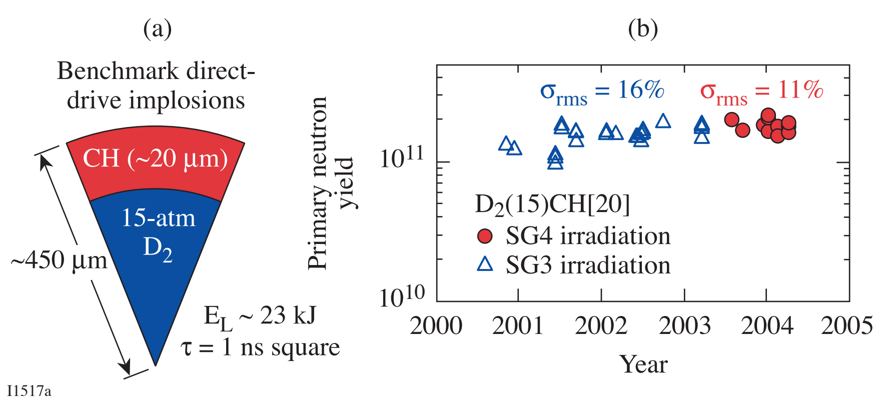

FIG. 1. (a) Schematic of a benchmark deuterium-filled plastic-shell target having a ~450-μm radius, a 20-μm shell thickness, and a 15-atm D_2 fill pressure. (b) The measured primary neutron yield of a benchmark target on OMEGA is highly reproducible over the last four years.

over clean (YOC). As shown in Fig. 2 the YOC for 3-atm-deuterium-filled, high-adiabat plastic-shell implosions with 27-μm-thick shells increased by almost a factor of 2 with the reduced low-ℓ-mode nonuniformity, while the YOC for the 20-μm-thick shells remained unchanged. The target performance of the unstable, thinner shell target is not sensitive to the reduced low-ℓ-mode nonuniformities because it is dominated by the single-beam-irradiation nonuniformities. However, the thicker shell target is less susceptible to the laser imprint and sensitive to the reduction in the low-ℓ-mode nonuniformities.

The RTI growth rate is expressed as $\gamma = \alpha_{RT}\sqrt{kg} - \beta_{RT}kV_a$, where $\alpha_{RT} = 0.94$ and $\beta_{RT} = 2.6$ for a DT ablator, k is the perturbation wave number, g is the acceleration, and the ablation velocity V_a is proportional to $\alpha^{3/5}$ [31]. Increasing α at the ablation surface reduces γ. However, α at the inner portion of the shell determines the minimum energy required for ignition $E_{min} \sim \alpha^{1.88}$ [32,33]. If α is uniform through the shell, there is a trade-off between target gain and stability. This trade-off can be avoided by tailoring the adiabat of the shell to optimize γ and E_{min}. By shaping the adiabat α of the shell, the value of α is raised at the ablation surface, increasing V_a and reducing γ, and is kept low in the inner portion of the shell, maintaining the compressibility of the target and maximizing the yield [34]. Adiabat shaping is achieved by launching an unsuppored shock wave into the shell with a short (~100-ps), intense Gaussian laser pulse ("picket") at the beginning of the implosion [34]. Alternatively, the adiabat can be shaped by relaxing the shell density with a weak laser prepulse, followed by a power shut-off prior to the foot of the main laser drive pulse [35,36].

Planar RTI x-ray radiography experiments were performed with a warm surrogate foam target overcoated with a thin layer of plastic [see Fig. 3(a)] to investigate the effect of the picket pulse on laser imprint [37]. The foils were driven with either the low-adiabat pulse shape without the picket or with the picket shown in Fig. 3(b). The measured radiographs show significant imprint reduction with picket pulses [see Fig. 3(c)]. Figure 3(d) shows that the optical-depth modulations are significantly reduced at shorter wavelengths using a picket pulse.

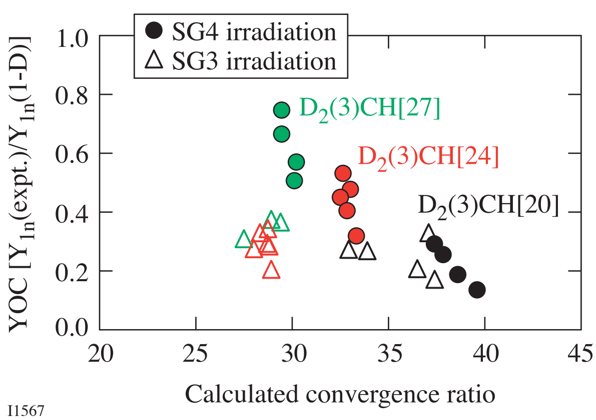

FIG. 2. The ratio of measured primary neutron yield to the 1-D predicted yield (YOC) for 3-atm-deuterium-filled, high-adiabat plastic-shell implosions is plotted as a function of the calculated convergence ratio for the SG3 and SG4 irradiation conditions. The new SG4 phase plate design with n = 4.1 replaced the SG3 design with n = 2.2, resulting in a reduction in the on-target laser irradiation nonuniformities for $\ell \leq 10$ by almost a factor of two.

3. Symmetric Illumination Direct-Drive Ignition Designs

Ignition target designs are being validated with implosions on OMEGA. Cryogenic and plastic/foam (surrogate-cryogenic) targets that are hydrodynamically scaled from ignition target designs (laser energy ~ target radius^3, laser power ~ target radius^2, and time ~ target radius) are imploded on OMEGA to investigate the key target physics issues of energy coupling, hydrodynamic instabilities, and implosion symmetry [5,15,38,39]. Schematics of the all-DT, $\alpha = 3$, direct-drive ICF ignition target design for the NIF, and the OMEGA $\alpha = 4$, cryogenic deuterium layered target design are shown in Fig. 4, along with the laser pulse shapes. Preheat of the fuel by fast electrons generated by the two-plasmon-decay instability and radiation from the corona can adversely affect target performance. Measurements of preheat due to fast electrons in laser implosions show that about 0.3% of incident laser energy is deposited as preheat due to fast electrons, which is within acceptable limits for direct-drive ICF [40].

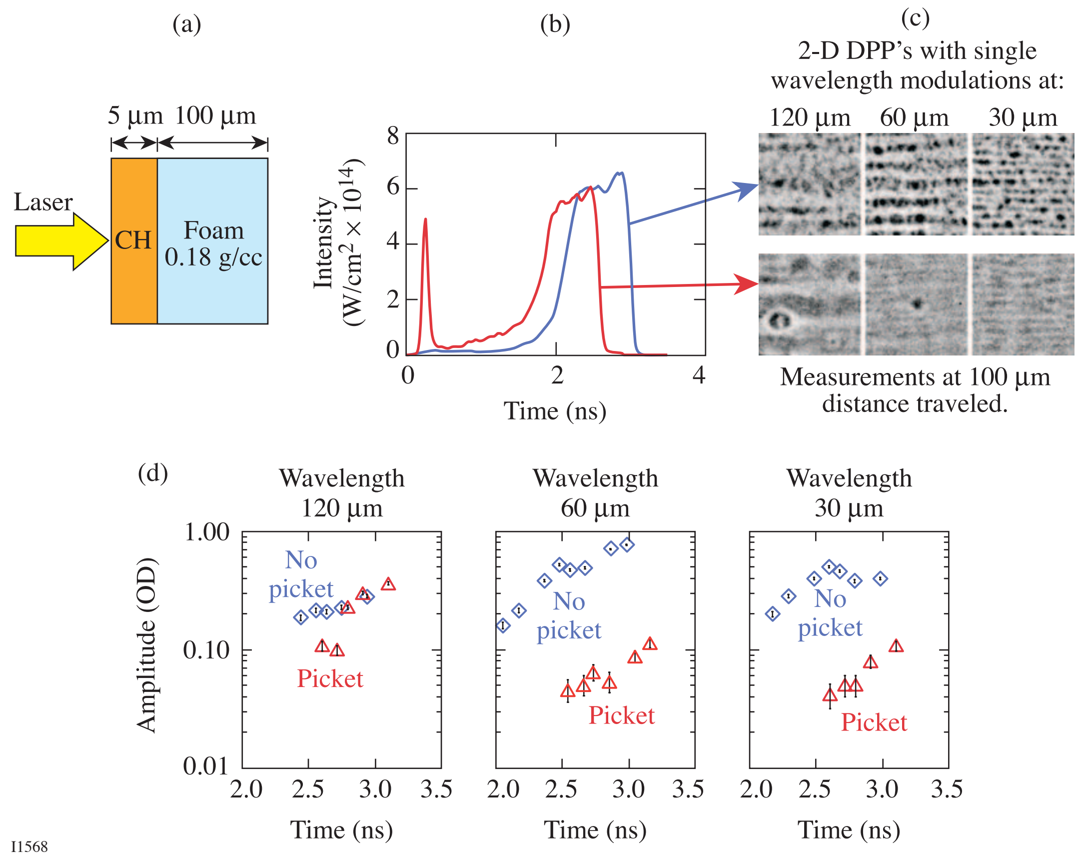

FIG. 3. (a) Warm surrogate foam target used in planar RTI x-ray radiography experiment investigating the effects of the picket; (b) low-adiabat laser pulse shapes with and without the picket. (c) Measured radiographs show significant laser imprint reduction with the picket pulse. (d) Optical-depth modulations are significantly reduced at shorter wavelengths using the picket pulse.

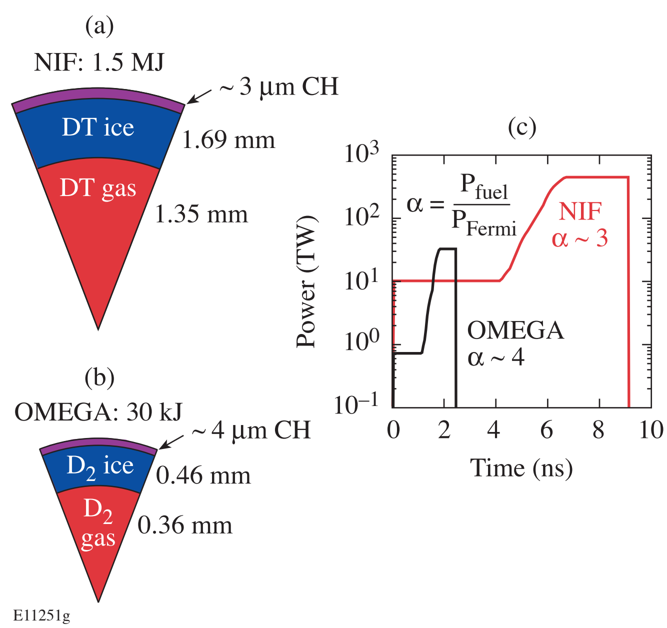

FIG. 4. Schematics of (a) the all-DT, $\alpha = 3$, direct-drive ICF ignition target design developed at LLE for the NIF and (b) the OMEGA $\alpha = 4$, cryogenic deuterium layered target design, along with (c) the laser pulse shapes.

Routine cryogenic target implosions have required significant engineering and development. Cryogenic implosions have been carried out on OMEGA for the last three years. Significant obstacles have been overcome, including cryogenic target transport, target survival, target-layer survival, and target vibration at shot time. Recently, eight cryogenic targets were shot in a single week. In a cryogenic target, perturbations of the inner ice surface also seed the RTI both by feedout during the acceleration phase and by directly seeding the deceleration phase. Extensive research and development has produced ice-layer finishes [41] approaching the 1-μm NIF requirement for ignition targets. The inner ice roughness is characterized using shadowgraphy [42]. A shadowgraph of a cryogenic layer target is shown in Fig. 5(a). The experimental signature of the inner ice roughness is the radial location of the bright band that can be observed in the unwrapped image of Fig. 5(b). The mode spectrum of the inner ice roughness shown in Fig. 5(c) is calculated from this feature. The smoothest layers with ~1-μm rms roughness were confined to localized regions of the target. A 3-D reconstruction of the inner ice layer is constructed from many views of the target, and low-order ℓ and m modes of the inner ice surface are calculated [41]. Structures in the ice correlate with known asymmetries in the layering spheres and are consistent over repeated layering/melting cycles.

The performance of imploded cryogenic D_2 capsules on OMEGA is close to the predictions of the 2-D hydrodynamics code *DRACO* [5,39]. As shown in Fig. 6, the 2-D predicted YOC

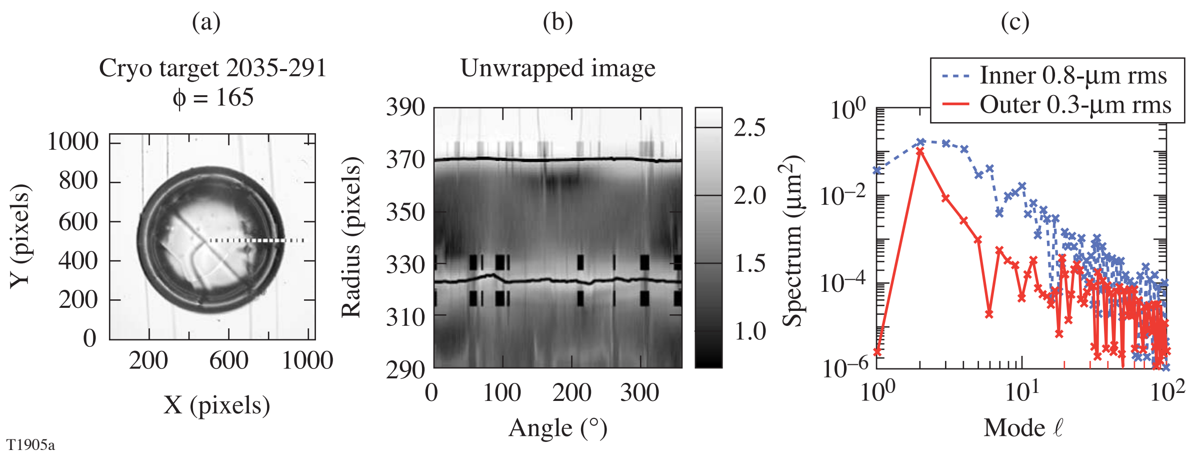

FIG. 5. The inner ice roughness is characterized using shadowgraphy. (a) A shadowgraph of a cryogenic layer target. (b) The unwrapped image of the shadowgraph shows the radial location of the bright band that is used to evaluate the mode spectrum of the inner ice roughness. (c) mode spectrum of inner ice roughness.

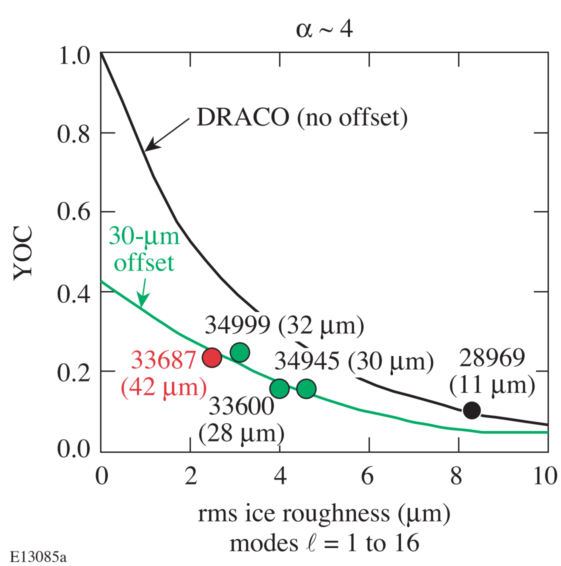

FIG. 6. A comparison of the 2-D-predicted YOC with the experimentally determined YOC for low-adiabat cryogenic implosions.

shows good agreement with the experimentally determined YOC over a wide range of ice roughness and target offset conditions for the $\alpha \sim 4$ implosions. The target-positioning offsets are primarily due to vibration. Uniform laser irradiation of the target is achieved when it is located at target chamber center; hence, offsets cause low-ℓ-mode irradiation nonuniformities. These vibrations will be reduced to negligible levels with a new, more-robust mechanical support. The average measured $\rho R \sim 50$ mg/cm^2 is 80% of 1-D predictions and very close to 2-D predictions. In addition, the hot spot n_e and T_e profiles of an imploded cryogenic D_2 target were inferred with gated x-ray core images and secondary neutron measurements and are close to 1-D predictions [43]. The inferred isobaric core pressure is ~5 Gbar.

The effects of laser irradiation nonuniformities and target surface roughness on implosion performance are modeled with the 2-D hydrodynamics code *ORCHID* or *DRACO* [5,6]. The sources for nonuniformity are (1) laser imprint associated with two-color cycle × 1-THz 2-D SSD, (2) on-target power imbalance, (3) inner-surface roughness of the ice layer, and (4) outer-surface roughness of the capsule. At the end of the acceleration phase the predicted distortions on the inner ice surface due to the hydrodynamic instabilities are quantified with the parameter $\bar{\sigma}$ [6], a weighted sum of the inner-ice-surface power spectra given by

$$\bar{\sigma} = \sqrt{0.06 \times \bar{\sigma}_\ell^2(\ell < 10) + \bar{\sigma}_\ell^2(\ell \geq 10)}.$$

These distortions are the major source of perturbations contributing to the seed for the deceleration-phase RTI. A scaling of gain versus $\bar{\sigma}$ was established using 2-D *ORCHID* burn calculations. The $\bar{\sigma}$ scaling has been used to predict the yield of the $\alpha = 4$ OMEGA cryogenic implosion. The performance of the all-DT, $\alpha = 3$ NIF direct-drive target design and the $\alpha = 4$ OMEGA cryogenic implosion predicted using the $\bar{\sigma}$ scaling is presented in Fig. 7. The vertical lines in Fig. 7 are the calculated values of $\bar{\sigma}$ for laser irradiation conditions of 1-THz, 2-D SSD with PS and 1% rms power imbalance, and target quality of 1-μm rms inner ice roughness and 840 Å outer-surface roughness. The $\bar{\sigma}$ scaling shows good agreement with the measured performance of the $\alpha = 4$ OMEGA cryogenic implosions (Fig. 7). Improvements in laser irradiation uniformity and target quality on OMEGA are expected to increase the normalized yield (YOC) to ~0.4. Using the $\bar{\sigma}$ scaling with yield allows the experimental validation of the numerical modeling of current OMEGA experiments and gives confidence in the ability of these numerical models to predict ignition for direct-drive target designs on the NIF. The 2-D predicted gain of the all-DT, $\alpha = 3$ NIF direct-drive target design is ~30. Adiabat shaping boosts the stability of this design and increases the 2-D predicted gain to 35.

The path to ignition involves DT cryogenic implosions. To this end a new D_2 fill and transfer station (FTS) is presently under construction to provide concurrent DT and D_2 cryogenic operations on OMEGA. Initial cryogenic DT implosions are expected in spring 2005.

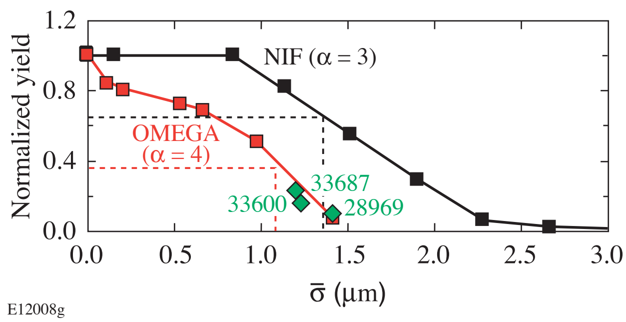

FIG. 7. The performance of the all-DT, $\alpha = 3$ NIF direct-drive target design and the $\alpha = 4$ OMEGA cryogenic implosion predicted using the $\bar{\sigma}$ scaling. The vertical lines are the expected values of $\bar{\sigma}$ on NIF and OMEGA. The measured performance of the $\alpha = 4$ OMEGA cryogenic implosions are the green diamonds.

4. Polar Direct Drive on the NIF and OMEGA

Prospects for direct-drive ignition on the NIF while it is configured in its x-ray-drive irradiation configuration are favorable with polar direct-drive (PDD) [8]. The PDD approach is based on the optimization of phase-plate design, beam pointing, and pulse shaping. The baseline PDD design uses a scaled-down version of a NIF high-performance, wetted-foam, direct-drive target design. The equivalent 1-D design absorbs 95% of the 1.1 MJ incident on the target. It has an implosion velocity of 4×10^7 cm/s, a peak ρR of 1.2 g/cm^2, and a gain of 54. Figure 8 shows the standard pointing with x-ray drive configuration in (a), the repointing for PDD in (b) and a contour plot of the mass density at peak burn from a 2-D hydrodynamic simulation in (c). The PDD target design has a 2-D predicted gain of ~10. It trades high gain for increased laser irradiation nonuniformity.

PDD simulations are being validated by experiments on OMEGA. The NIF PDD configuration with 48 quads was approximated by repointing 40 beams of OMEGA. Experiments on OMEGA measured the nonuniformities in the imploding shell. As shown in Fig. 9, computer simulations

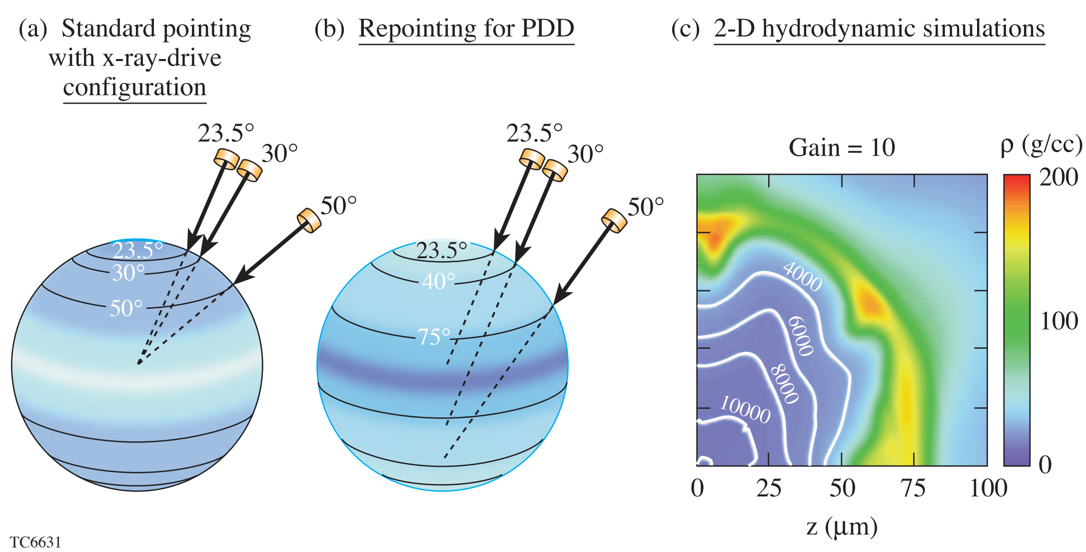

FIG. 8. (a) The standard pointing with x-ray-drive configuration, (b) the repointing for PDD, and (c) a contour plot of the mass density at peak burn from a 2-D hydrodynamic simulation. The PDD target design has a 2-D predicted gain of ~10.

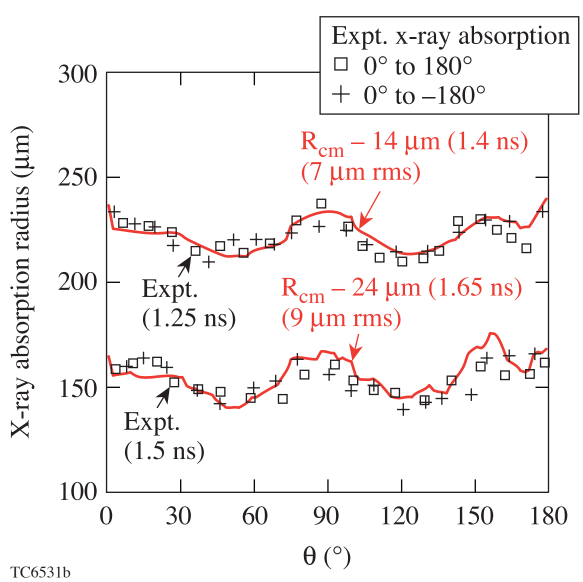

FIG. 9. A comparison of the measured nonuniformities (black symbols) in the imploding shell of a PDD target on OMEGA with the simulation (red curves).

track the measured target nonuniformity quite well. In addition, *DRACO* simulations of x-ray emission from the PDD experiments reproduce the qualitative shape of the compressed core.

5. Fast-Ignition Research on OMEGA

Fast ignition (FI) is an active area of research at LLE [9]. Higher gains are predicted with FI than with hot-spot ignition; consequently, ignition could be achieved at lower drive energies. A high-energy petawatt (HEPW) capability is being constructed at LLE next to the existing 60-beam OMEGA facility. The OMEGA EP (extended performance) laser will add two short-pulse, 2- to 3-PW, 2.6-kJ beams to the OMEGA laser system to study FI physics with focused intensities up to 6×10^{20} W/cm^2. The HEPW beams will be integrated into the OMEGA compression facility for experiments beginning in 2008. Experiments designed to validate fast ignition will be performed with scaled cryogenic capsules. A high-density fuel configuration will be assembled with the OMEGA compression facility, and the OMEGA EP will produce suprathermal electrons via high-intensity laser–plasma interaction to heat the core. Radiographic diagnostic capability will be developed with OMEGA EP for cryogenic implosions with high fuel areal densities, and for high energy density physics relevant experiments on the NIF [44].

Surrogate direct-drive fuel-assembly experiments with FI cone targets have been performed on OMEGA, and a substantial fraction of the predicted core areal density was measured. Gas-tight FI targets with a Au cone developed for fuel-assembly experiments [45] [see Fig. 10(a)] were imploded on OMEGA [46]. The Au cone had a 35° half-angle. The target was filled with 10 atm of D_2 or D^3He. The plastic shell had a 24-μm-thick wall and an 870-μm outside diameter. As shown in Fig. 10(b) the backlit framing-camera images show the core assembly and cone reaction in great detail. A neutron-burn-averaged $\rho R \sim 60$ mg/cm^2 was inferred from the energy loss of the D^3He protons [17].

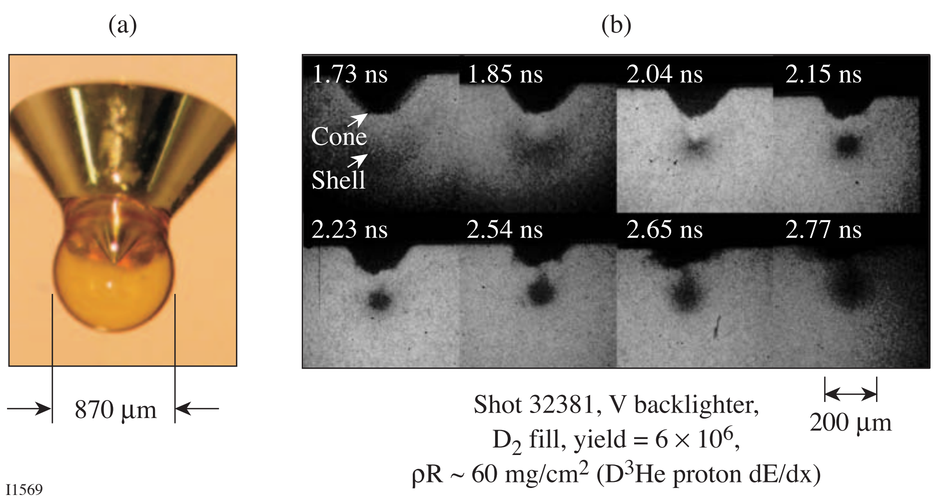

FIG. 10. (a) A gas-tight FI target with a Au cone developed for fuel-assembly experiments was imploded on OMEGA. (b) Backlit x-ray-framing-camera images show the core assembly and cone reaction in great detail.

6. Conclusions

In conclusion, the achievement of thermonuclear ignition with direct-drive on the NIF is extremely promising. Significant experimental and theoretical progress has been achieved by LLE's direct-drive ICF program, charting the path to ignition. High-performance layered deuterium cryogenic targets are imploded on OMEGA to validate the hydrodynamics codes used to design direct-drive ignition targets. Initial cryogenic DT implosions are expected on OMEGA in the spring of

2005. Symmetric direct-drive on the NIF is predicted to achieve high gain (~35) with adiabat shaping. Prospects for direct-drive on the NIF while it is in its x-ray-drive irradiation configuration are also extremely favorable with polar direct-drive having a predicted gain ~10. Fully integrated fast-ignition experiments will begin on the OMEGA compression facility once the high-energy petawatt upgrade—OMEGA EP—is completed.

Acknowledgment

This work was supported by the U.S. Department of Energy Office of Inertial Confinement Fusion under Cooperative Agreement No. DE-FC03-92SF19460, the University of Rochester, and the New York State Energy Research and Development Authority. The support of DOE does not constitute an endorsement by DOE of the views expressed in this article.

References

[1] SETHIAN, J.D., et al., "Fusion energy with lasers, direct drive targets, and dry wall chambers", Nucl. Fusion **43** (2003) 1693–1709.

[2] LINDL, J.D., *Inertial Confinement Fusion: The Quest for Ignition and Energy Gain Using Indirect Drive*, Springer-Verlag, New York (1998).

[3] MCCRORY, R.L., et al., "Progress in direct-drive inertial confinement fusion research at the Laboratory for Laser Energetics", Nucl. Fusion (to be published).

[4] PAISNER, J., et al., "National Ignition Facility would boost US industrial competitiveness", Laser Focus World **30** (1994) 75–77.

[5] MCKENTY, P.W., et al., "Direct-drive cryogenic target implosion performance on OMEGA", Phys. Plasmas **11** (2004) 2790–2797.

[6] MCKENTY, P.W., et al., "Analysis of a direct-drive ignition capsule designed for the National Ignition Facility", Phys. Plasmas **8** (2001) 2315–2322.

[7] BOEHLY, T.R., et al., "Initial performance results of the OMEGA laser system", Opt. Commun. **133** (1997) 495–506.

[8] SKUPSKY, S., et al., "Polar direct drive on the National Ignition Facility", Phys. Plasmas **11** (2004) 2763–2770.

[9] TABAK, M., et al., "Ignition and high gain with ultrapowerful lasers", Phys. Plasmas **1** (1994) 1626–1634.

[10] Bodner, S.E., et al., "Direct-drive laser fusion: Status and prospects", Phys. Plasmas **5** (1998) 1901–1918.

[11] REGAN, S.P., et al., "Dependence of shell mix on feedthrough in direct drive inertial confinement fusion", Phys. Rev. Lett. **92** (2004) 185002.

[12] REGAN, S.P., et al., "Shell mix in compressed core of spherical implosions", Phys. Rev. Lett. **89** (2002) 085003.

[13] BELL, G.I., "Taylor instability on cylinders and spheres in the small amplitude approximation", Los Alamos National Laboratory, Los Alamos, NM, Report LA-1321 (1951).

[14] PLESSET, M.S., "On the stability of fluid flows with spherical symmetry", J. Appl. Phys. **25** (1954) 96–98.

[15] MEYERHOFER, D.D., et al., "Core performance and mix in direct-drive spherical implosions with high uniformity", Phys. Plasmas **8** (2001) 2251–2256.

[16] Li, C.K., et al., "Effects of fuel-shell mix upon direct-drive, spherical implosions on OMEGA", Phys. Rev. Lett. **89** (2002) 165002.

[17] SÉGUIN, F.H., et al., "Spectrometry of charged particles from inertial-confinement-fusion plasmas", Rev. Sci. Instrum. **74** (2003) 975–995.

[18] REGAN, S.P., et al., "Characterization of direct-drive-implosion core conditions on OMEGA with time-resolved Ar *K*-shell spectroscopy", Phys. Plasmas **9** (2002) 1357–1365.

[19] SMALYUK, V.A., et al., "Evolution of shell nonuniformities near peak compression of spherical implosion", Phys. Rev. Lett. **87** (2001) 155002.

[20] SKUPSKY, S., CRAXTON, R.S., "Irradiation uniformity for high-compression laser-fusion experiments", Phys. Plasmas **6** (1999) 2157–2163.

[21] SKUPSKY, S., et al., "Improved laser-beam uniformity using the angular dispersion of frequency-modulated light", J. Appl. Phys. **66** (1989) 3456–3462.

[22] ROTHENBERG, J.E., "Comparison of beam-smoothing methods for direct-drive inertial confinement fusion", J. Opt. Soc. Am. B **14** (1997) 1664–1671.

[23] REGAN, S.P., et al., "Experimental investigation of smoothing by spectral dispersion", J. Opt. Soc. Am. B **17** (2000) 1483–1489.

[24] KESSLER, T.J., et al., "Phase conversion of lasers with low-loss distributed phase plates", in *Laser Coherence Control: Technology and Applications*, POWELL, H.T., KESSLER, T.J. (Eds.), Vol. 1870, SPIE, Bellingham, WA (1993), 95–104.

[25] LIN, Y., KESSLER, T.J., LAWRENCE, G.N., "Design of continuous surface-relief phase plates by surface-based simulated annealing to achieve control of focal-plane irradiance", Opt. Lett. **21** (1996) 1703–1705.

[26] KATO, Y., unpublished notes from work at LLE, 1984; TSUBAKIMOTO, K., et al., "Suppression of interference speckles produced by a random phase plate, using a polarization control plate", Opt. Commun. **91** (1992) 9–12; TSUBAKIMOTO, K., et al., "Suppression of speckle contrast by using polarization property on second harmonic generation", Opt. Commun. **103** (1993) 185–188.

[27] "Phase conversion using distributed polarization rotation", Laboratory for Laser Energetics LLE Review **45**, 1–12, NTIS document No. DOE/DP40200-149 (1990). Copies may be obtained from the National Technical Information Service, Springfield, VA 22161; GUNDERMAN, T.E., et al., "Liquid crystal distributed polarization rotator for improved uniformity of focused laser light", in *Conference on Lasers and Electro-Optics*, Vol. 7, 1990 OSA Technical Digest Series, Optical Society of America, Washington, DC (1990), 354.

[28] BOEHLY, T.R., et al., "Reduction of laser imprinting using polarization smoothing on a solid-state fusion laser", J. Appl. Phys. **85** (1999) 3444–3447.

[29] MARSHALL, F.J., et al., "Direct-drive-implosion experiments with enhanced fluence balance on OMEGA", Phys. Plasmas **11** (2004) 251–259.

[30] "Performance of 1-THz-bandwidth, 2-D smoothing by spectral dispersion and polarization smoothing of high-power, solid-state laser beams", Laboratory for Laser Energetics LLE Review **98**, 49–53, NTIS document No. DOE/SF/19460-527 (2004). Copies may be obtained from the National Technical Information Service, Springfield, VA 22161, and J. Opt. Soc. Am. B (to be published).

[31] BETTI, R., et al., "Growth rates of the ablative Rayleigh–Taylor instability in inertial confinement fusion", Phys. Plasmas **5** (1998) 1446–1454.

[32] HERRMANN, M.C., TABAK, M., LINDL, J.D., "Ignition scaling laws and their application to capsule design", Phys. Plasmas **8** (2001) 2296–2304.

[33] BETTI, R., et al., "Deceleration phase of inertial confinement fusion implosions", Phys. Plasmas **9** (2002) 2277–2286.

[34] GONCHAROV, V.N., et al., "Improved performance of direct-drive inertial confinement fusion target designs with adiabat shaping using an intensity picket", Phys. Plasmas **10** (2003) 1906–1918.

[35] ANDERSON, K., BETTI, R., "Laser-induced adiabat shaping by relaxation in inertial fusion implosions", Phys. Plasmas **11** (2004) 5–8.

[36] ANDERSON, K., BETTI, R., "Theory of laser-induced adiabat shaping in inertial fusion implosions: The decaying shock", Phys. Plasmas **10** (2003) 4448–4462.

[37] KNAUER, J.P., et al., "Improved target stability using picket pulses to increase and shape the ablator adiabat", Phys. Plasmas (to be submitted).

[38] STOECKL, C., et al., "First results from cryogenic target implosions on OMEGA", Phys. Plasmas **9** (2002) 2195–2201.

[39] SANGSTER, T.C., et al., "Direct-drive cryogenic target implosion performance on OMEGA", Phys. Plasmas **10** (2003) 1937–1945.

[40] YAAKOBI, B., et al., "Measurement of preheat due to fast electrons in laser implosions", Phys. Plasmas **7** (2000) 3714–3720.

[41] MEYERHOFER, D.D., et al., "Cryogenic target characterization at LLE", Bull. Am. Phys. Soc. **48** (2003) 55.

[42] KOCH, J.A., et al., "Numerical raytrace verification of optical diagnostics of ice surface roughness for inertial confinement fusion experiments", Fusion Sci. Technol. **43** (2003) 55–66.

[43] SMALYUK, V.A., et al., "Hot-core characterization of the cryogenic D_2 target at peak neutron production in direct-drive spherical implosion", Phys. Rev. Lett. (submitted).

[44] NATIONAL RESEARCH COUNCIL (U.S.) COMMITTEE on High Energy Density Plasma Physics, *Frontiers in High Energy Density Physics: The X-Games of Contemporary Science*, National Academies Press, Washington, DC (2003).

[45] Targets were produced by General Atomics, San Diego, CA 92121-1122.

[46] STOECKL, C., et al., "Fuel assembly experiments with gas-filled, cone-in-shell, fast-ignitor targets on OMEGA", Phys. Rev. Lett. (submitted).